Biochemical and Biophysical Research Communications 401 (2010) 143–148

Contents lists available at ScienceDirect

Biochemical and Biophysical Research Communications

journal homepage: www.elsevier.com/locate/ybbrc

AHNAK1 and AHNAK2 are costameric proteins: AHNAK1 affects transverse skeletal muscle fiber stiffness

Andreas Marg [a,*], Hannelore Haase [a], Tanja Neumann [b], Michiyoshi Kouno [c], Ingo Morano [a,d]

[a] Max-Delbrück-Centrum für Molekulare Medizin, D-13092 Berlin, Germany
[b] JPK Instruments AG, Bouchéstrasse 12, D-12435 Berlin, Germany
[c] School of Medicine, Keio University, 35 Shinanomachi, Shinjuku, Tokyo 160-8582, Japan
[d] University Medicine Charité, Berlin, Germany

ARTICLE INFO

Article history:
Received 3 September 2010
Available online 15 September 2010

Keywords:
AHNAK1
AHNAK2
Costamer
Fiber stiffness
Membrane repair
Skeletal muscle

ABSTRACT

The AHNAK scaffold PDZ-protein family is implicated in various cellular processes including membrane repair; however, AHNAK function and subcellular localization in skeletal muscle are unclear. We used specific AHNAK1 and AHNAK2 antibodies to analyzed the detailed localization of both proteins in mouse skeletal muscle. Co-localization of AHNAK1 and AHNAK2 with vinculin clearly demonstrates that both proteins are components of the costameric network. In contrast, no AHNAK expression was detected in the T-tubule system. A laser wounding assay with AHNAK1-deficient fibers suggests that AHNAK1 is not involved in membrane repair. Using atomic force microscopy (AFM), we observed a significantly higher transverse stiffness of AHNAK1$^{-/-}$ fibers. These findings suggest novel functions of AHNAK proteins in skeletal muscle.

1. Introduction

The AHNAK family of scaffold PDZ proteins consists of two large proteins (600–700 kD), AHNAK1 (desmoyokin) and AHNAK2 [1–3]. Scaffold proteins interact with various proteins and can link cytoskeleton to the plasma membrane or transmit extracellular signals to intracellular acceptors [4]. The AHNAK1 structure can be divided into three main regions: the NH2-terminal part with about 500 amino acids, a large central region of 4390 amino acids composed of a 128 amino acid unit repeated 26 times, and a COOH-terminal part with 1002 amino acids. Both AHNAK proteins have a predicted PDZ domain with unknown function in the N-terminal region of the protein [1]. There is no evidence for the presence of transmembrane domains in AHNAK sequences.

High expression levels of AHNAK1 were found in all muscular cells including cardiomyocytes and skeletal muscle cells [5]. AHNAK1 expression was also discovered in epithelial cells and in T-cells. In adult tissues, the main localization of AHNAK1 is at the plasma membrane. On sections of skeletal muscles, a not further characterized AHNAK1 expression at the sarcolemma was found [5,6]. In cardiomyocytes, AHNAK1 is strictly localized to the inner aspect of the sarcolemma, intercalated disc, and T-tubular system [7]. Up to now, the cellular localization of AHNAK2 in skeletal muscle is unknown.

Through protein–protein interactions AHNAK1 is involved in calcium signaling. In cardiomyocytes, AHNAK1 is phosphorylated by protein kinase A and associates with the β-subunit of cardiac Ca(v) calcium channel [8]. In peripheral CD4^{+} T cells, AHNAK1 mediates the regulation of calcium signaling through Cav1.1 α1 subunits [9]. The function of AHNAK protein family in skeletal muscle fibers is widely unknown. In vitro studies give evidence for interactions between dysferlin and AHNAK and between myoferlin and AHNAK in skeletal muscles [6]. The authors also assume the involvement of AHNAK proteins in membrane repair.

2. Materials and methods

2.1. Mice

AHNAK1$^{-/-}$ mice and attendant wt mice were described previously [10].

2.2. Isolation of single muscle fibers

Single muscle fibers were isolated from *flexor digitorum brevis* (FDB) of 12 week old male mice by treatment with type I collagenase (0.5 mg/ml, Lot S8C10400, Worthington) in Minimal Essential

Abbreviations: AFM, atomic force microscopy; FDB, *flexor digitorum brevis*; LSM, laser scanning microscopy; wt, wild type.

* Corresponding author. Address: Max-Delbrück-Centrum für Molekulare Medizin (MDC), Robert-Rössle-Str. 10, 13092 Berlin, Germany. Fax: +49 30 9406 2579.
E-mail address: andreas.marg@mdc-berlin.de (A. Marg).

0006-291X/$ - see front matter © 2010 Elsevier Inc. All rights reserved.
doi:10.1016/j.bbrc.2010.09.030

Medium Eagle (MEM, PAA) with 10% fetal calf serum and antibiotics. After incubation for 3 h at 37 °C, the FDB muscles were dissociated into single fibers by gently pipetting. Dissociated fibers were washed and resuspended in complete MEM and plated on laminin-coated coverslips.

2.3. Antibodies

Affinity-purified rabbit polyclonal antibodies were generated against AHNAK1 and AHNAK2. The AHNAK1 antibody was raised against a recombinant protein encoding C-terminal amino acids 4893–5535 [8] of human AHNAK1 (UniProtKB accession number: Q09666). This antibody detects both human and mouse AHNAK1. A peptide antibody against AHNAK2 was made using an epitope (GSEAMVASSARTEL) corresponding to amino acids 737–750 of the C-terminal region of mouse AHNAK2 (UniProtKB accession number: Q3URZ6). This epitope is lacking in AHNAK1. For immunofluorescence staining on single muscle fibers, both AHNAK antibodies were used in a concentration of 5 μg/ml. Monoclonal anti-vinculin antibody (clone hVIN-1, Sigma–Aldrich) was applied in a concentration of 5 μg/ml. Monoclonal anti-α-actinin antibody (clone EA-53) was also from Sigma–Aldrich. The ascites fluid was used in a dilution of 1:2000. Monoclonal anti-myomesin antibody (MyBB78) was a kind gift from Peter van der Ven. The cell culture supernatant was used in a dilution of 1:500. Monoclonal antibody 8B7 against Ca(v) 1.1 was a kind gift from Wolfgang Nastainczyk and Franz Hofmann and was described previously [11]. The cell culture supernatant was applied in a dilution of 1:5000. Alexa Fluor 488 anti-mouse and Alexa Fluor 568 anti-rabbit secondary antibodies were purchased from Invitrogen and used in a concentration of 2 μg/ml.

2.4. Immunofluorescence and confocal microscopy

Single muscle fibers on laminin-coated coverslips were incubated over night in a humidified 5% CO_2 atmosphere. After incubation, muscle fibers were washed with PBS and fixed in a 3.7% formaldehyde–PBS solution for 15 min at RT, rinsed in PBS and permeabilized with 0.5% triton X-100 in PBS for 10 min. After repeated wash with PBS, blocking was arranged with 0.2% fish skin gelatin (Sigma) in PBS for 45 min. Primary antibody incubation was done overnight in PBS with 0.2% fish skin gelatin at 4 °C. After two washes with 0.1% Nonidet P40 (Roche) in PBS secondary antibody incubation was performed for 2 h at RT in PBS. After three washes with 0.1% Nonidet P40 in PBS coverslips were mounted in Aqua PolyMount (Polysciences). Images were collected using a Zeiss-LSM 510 Meta confocal microscope equipped with a 63× oil immersion lens, the 488-nm laser line of a 30-mW argon-laser and the 561-nm laser line of a 15-mW DPSS-laser. Digital images were processed using Zeiss LSM Image Browser software.

2.5. Membrane repair assay

Single muscle fibers from wt- or AHNAK1$^{-/-}$ mice, isolated as described before, were plated onto laminin-coated μ-Slide 8 well (ibidi) in Tyrode solution (140 mM NaCl, 5 mM KCl, 2.5 mM $CaCl_2$, 2 mM $MgCl_2$ and 10 mM HEPES, pH 7.2). Membrane repair assay was performed with slight modifications as published before

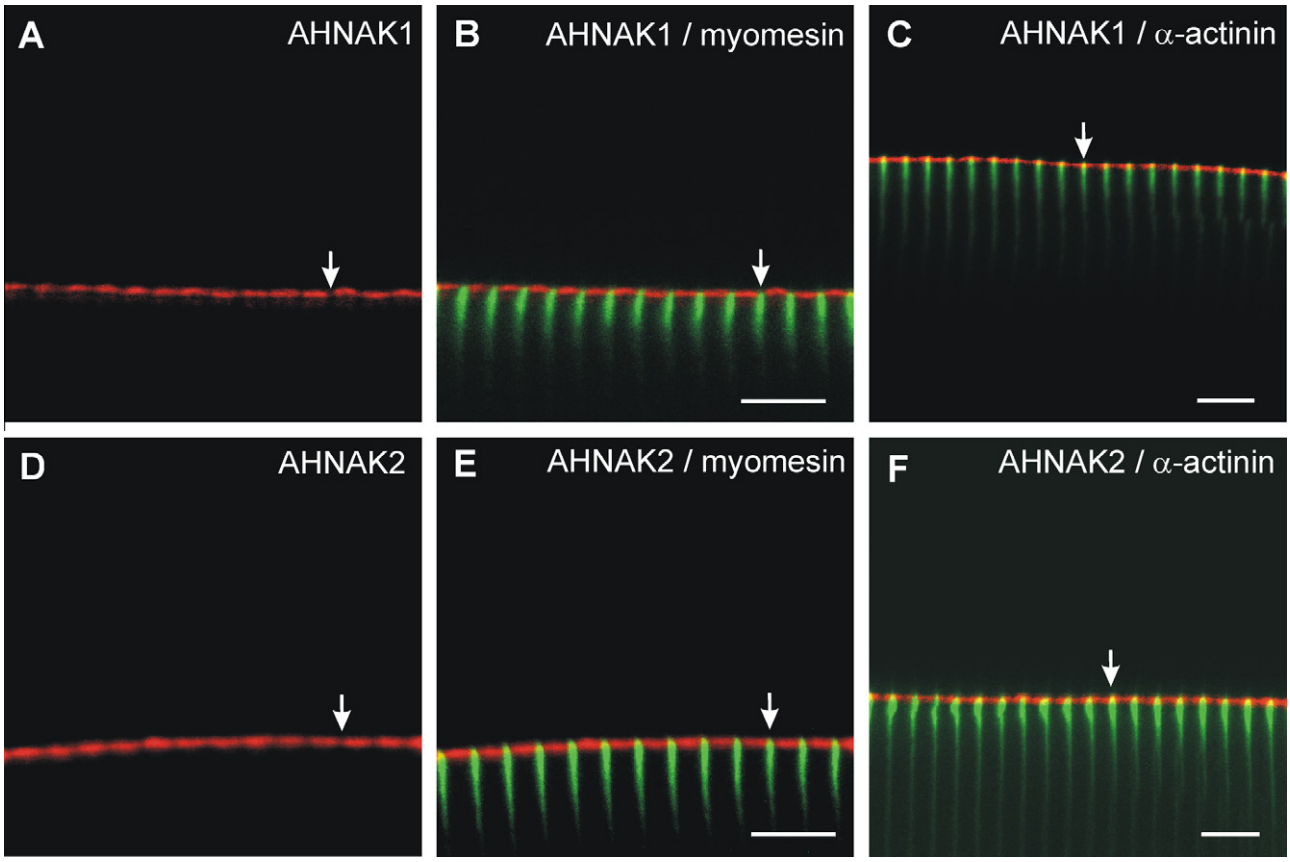

Fig. 1. AHNAK proteins are expressed in well differentiated structures near the sarcolemma. Single muscle fibers from the *flexor digitorum brevis* of 12-wk-old mice were stained for AHNAK1 (A) or AHNAK2 (D). The boundary areas of the fibers were analyzed using confocal microscopy. Co-staining of the same membrane region with myomesin (B and E) demonstrates a disruption of AHNAK expression pattern at the level of M-lines. Arrows indicate equal membrane position. A co-staining with α-actinin (C and F) shows a co-localization of AHNAK proteins and α-actinin in dot-like structures (yellow points) at the end of the Z-disks (arrows). Bars 5 μm.

[12]. To induce damage to the muscle fibers, a 5 × 5 μm boundary area of the fibers was irradiated at 50% maximum power (30-mW argon-laser) for 37 s using a Zeiss-LSM 510 META confocal microscope equipped with a 63× oil immersion lens. Experiments were done in Tyrode solution with 2.5 μM FM1-43FX (Molecular Probes). For Ca^{2+}-free experiments, $CaCl_2$ in Tyrode solution was replaced by 0.5 mM EGTA. Fibers which displayed a significant FM1-43 fluorescence before laser injury, were not used in the assay. Images were captured at 20-s intervals. To calculate the time-dependent fluorescence intensity, an area of 35 × 35 μm around the injury site was used and the initial fluorescence intensity was set to zero.

2.6. Atomic force microscopy

Atomic force spectroscopy measurements were performed using CellHesion 200 (JPK Instruments, Germany) mounted on an inverted optical microscope (Axio Observer D1, Carl Zeiss, Germany). Silicon tipless cantilevers (Arrow TL1, NanoWorld, Switzerland) with a nominal spring constant of 0.03 N/m were modified with 11 μm- glass spheres (Microparticles GmbH, Berlin; Coefficient of variation CV = 2%). The cantilever sensitivity and spring constant were determined using the in-built calibration routine (thermal noise method) [13]. Single muscle fibers, isolated as described above, were grown on laminin-coated Petri dishes for 48 h. Force measurements were performed in HEPES buffered DMEM/F12 (Invitrogen). To maintain the sample temperature at 37 °C, the Petri dishes were mounted on a PetriDishHeater (JPK Instruments, Germany). For force spectroscopy, the cantilever probe was positioned above the target fiber. Each fiber was tested at 5 different positions; 4 force-distance curves were taken on each position (20 curves per fiber). For more details on force spectroscopy see Supplementary Fig. 3. The cantilever speed was set to 0.5 μm/s, a setpoint of 2 nN was used. For force curve analysis the JPK Data Processing software was used. Force–distance curves were converted into force indentation curves by calculating the tip sample separation (corrects the distance for the cantilever deflection). The Young's modulus was determined for each force indentation curve by fitting the extend curves using the Hertz model for spherical indenters (diameter 11 μm; Poisson ratio 0.5) [14,15]. The fit range was set to 50 nm of indentation.

3. Results and discussion

3.1. AHNAK1 and AHNAK2 are costameric proteins

In initial experiments, we characterized the specificity of the AHNAK antibodies generated in this study. The AHNAK1 antibody shows a characteristic staining pattern on single FDB muscle fibers from wild type (wt) mice (Fig. S1A). A staining experiment on muscle fibers from AHNAK1$^{-/-}$ mice demonstrates that this antibody is specific for AHNAK1 and does not detect AHNAK2 (Fig. S1B). The AHNAK2 antibody, raised against a specific sequence lacking in AHNAK1, shows a distinctive staining on AHNAK1 knock out fibers (Fig. S1C). Summing up, antibodies used in our experiments are specific for AHNAK1 and AHNAK2 and are able to discriminate between these two proteins.

In the next set of experiments, we analyzed AHNAK1 and AHNAK2 expression in permeabilized single fibers from mouse skeletal muscles using laser scanning microscopy and observed continuous, intermittent pattern of immunostaining along the sarcolemma (Fig. 1A and D). Interestingly, this pattern appeared as expression spots described for the costameric protein dystrophin [16]. To further characterize the AHNAK expression, we used a co-staining of AHNAK1 and AHNAK2 with myomesin, which is a major compound of the M-line in striated muscles [17]. This staining

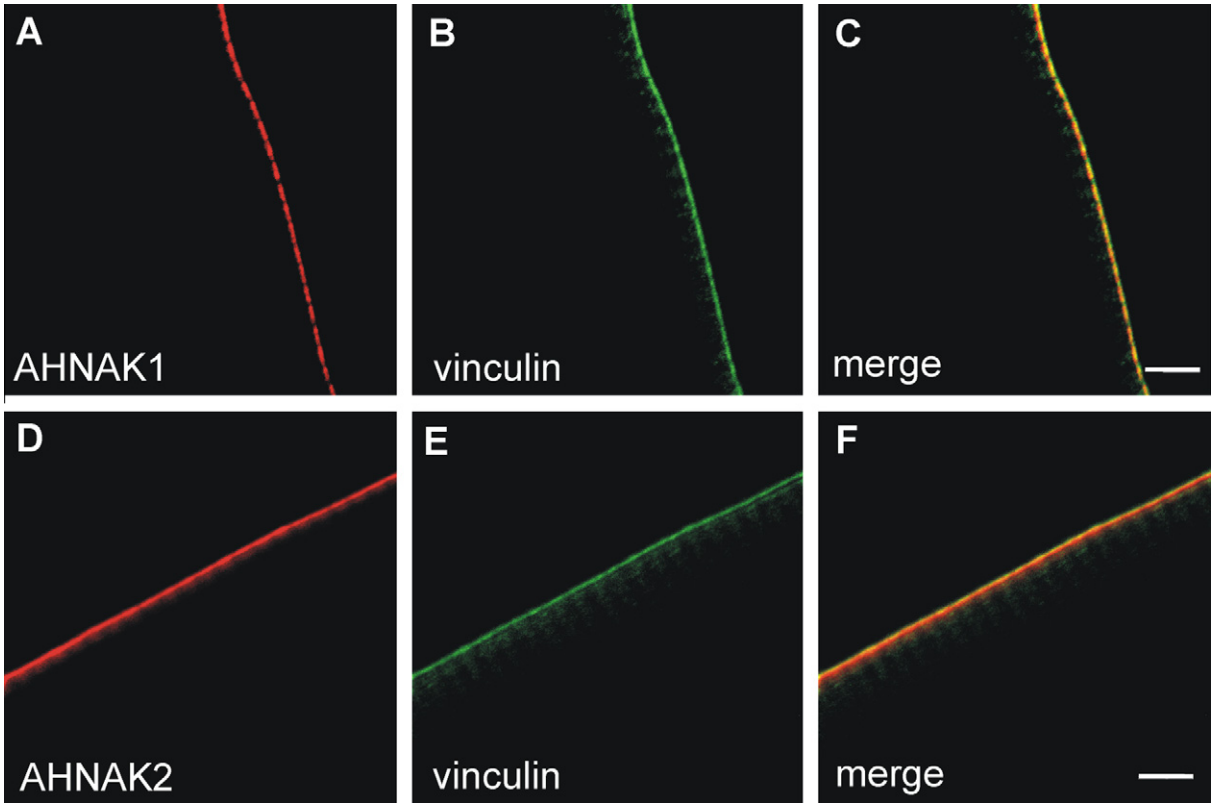

Fig. 2. AHNAK1 and AHNAK2 are co-localized with vinculin. Single FDB-fibers of 12-wk-old mice were stained for AHNAK1 (A), AHNAK2 (D) and vinculin (B and E). The overlays (C and F) clearly demonstrate a co-localization of AHNAK proteins with the costamere marker vinculin. Bars 5 μm.

demonstrates the disruption of the AHNAK expression at the level of M-lines of subsarcolemmal myofibrils (Fig. 1B and E). Furthermore, we examined the position of AHNAK expression pattern in relation to the Z-disks. In skeletal muscle fibers α-actinin is known as a protein localized to the Z-disks and to the costameres [18]. A co-staining of AHNAK1 and AHNAK2 with α-actinin clearly shows a dot-like co-localization of both AHNAK proteins with α-actinin in a region at the end of the Z-disks (Fig. 1C and F). No AHNAK staining was found at the Z-disks. These results justify the assumption that AHNAK1 and AHNAK2 are costameric proteins.

Costameres are subsarcolemmal protein assemblies in striated muscle cells first described by Pardo et al. [19]. Physically, they mediate the lateral transmission of force from the sarcomeres across the sarcolemma to the extracellular matrix. Structurally, costameres connect the Z-disks with the sarcolemma. Costameres are of particular importance to normal muscle function. The loss or defect of costameric proteins or their interacting partners in Z-disk or in sarcolemma often cause muscular dystrophies [20,18]. The focal adhesion protein vinculin, known to be a key element for the linkage of the extracellular matrix to the cytoplasmic microfilament system, is also a founding member of costameres [19]. Vinculin staining pattern have been used to identify many other costameric proteins in striated muscles. On this account, we also compared the AHNAK expression (Fig. 2A and D) with

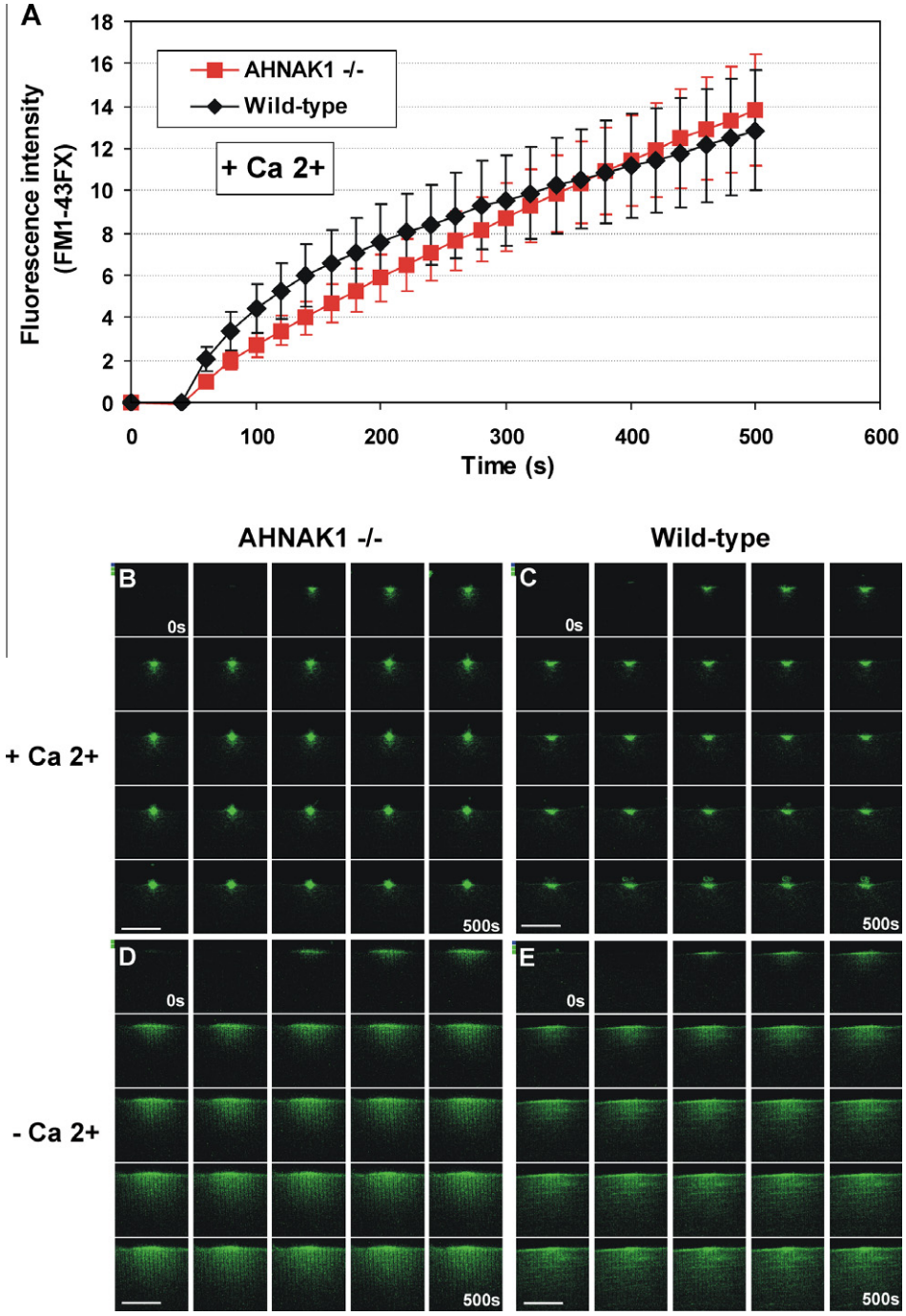

Fig. 3. Intact membrane repair in AHNAK1-deficient mice. (A) Time-dependent import of FM1-43FX into mouse FDB muscle fibers induced by laser damage of the sarcolemmal membrane in the presence of calcium. Data are means ± SEM of 12 wt fibers and 10 fibers from AHNAK1$^{-/-}$ mice. (B–E) Representative time-scans of single muscle fibers after laser wounding at 20-s intervals. The respective first chart (0s) was done before laser wounding. Controls (D and E) demonstrate unhindered import of FM1-43FX in the absence of calcium into wt- and AHNAK1$^{-/-}$ fibers. Bars 20 μm.

the expression pattern of the costameric marker protein vinculin (Fig. 2B and E) and find here an exact conformity in the overlay for AHNAK1 and AHNAK2 (Fig. 2C and F). These results clearly demonstrate that both AHNAK proteins are components of the costameric network and give new insights in the biological function of AHNAK in skeletal muscle.

Kouno et al. [10] and Komuro et al. [1] reported AHNAK1 homozygous knockouts which are normal in growth and development and show no obvious phenotype. We demonstrate here that AHNAK1 and AHNAK2 co-localize in the costameres in skeletal muscle and support the notion that AHNAK2 may replace AHNAK1 functionally in part or completely. A participation in the costameric network may also simply explain the localization of AHNAK proteins at the sarcolemma without direct anchoring in the membrane.

3.2. AHNAK is not expressed in T-tubules of muscle fibers

In cardiomyocytes, AHNAK proteins are localized at the sarcolemmal membrane and at transverse tubule membranes [1,7]. To clarify the AHNAK expression in the T-tubule system of adult skeletal muscles, we used a 14 μm-laser scanning microscopy (LSM)-scan through single muscle fibers (Fig. S2A and B). Surprisingly, we do not detect any AHNAK1- or AHNAK2 staining in T-tubules. To support our observation, we used a co-immunostaining of AHNAK2 with the T-tubule marker Ca_v 1.1 and find clearly different expression pattern of AHNAK2 and Ca_v 1.1 in skeletal muscle fibers (Fig. S2C). These results disagree with a previous publication [6], which describes an AHNAK co-localization with the dihydropyridine receptor (Ca_v 1.1) at the T-tubules of skeletal muscles. Our observation provides evidence for quite different functions of AHNAK proteins in calcium signaling of cardiomyocytes and skeletal muscles.

3.3. Intact membrane repair in AHNAK1-deficient mice

Huang et al. [6] proposed a role of AHNAK in membrane repair process of skeletal muscle fibers. We used AHNAK1$^{-/-}$ fibers in a laser-based membrane wounding assay [12,21] to verify this

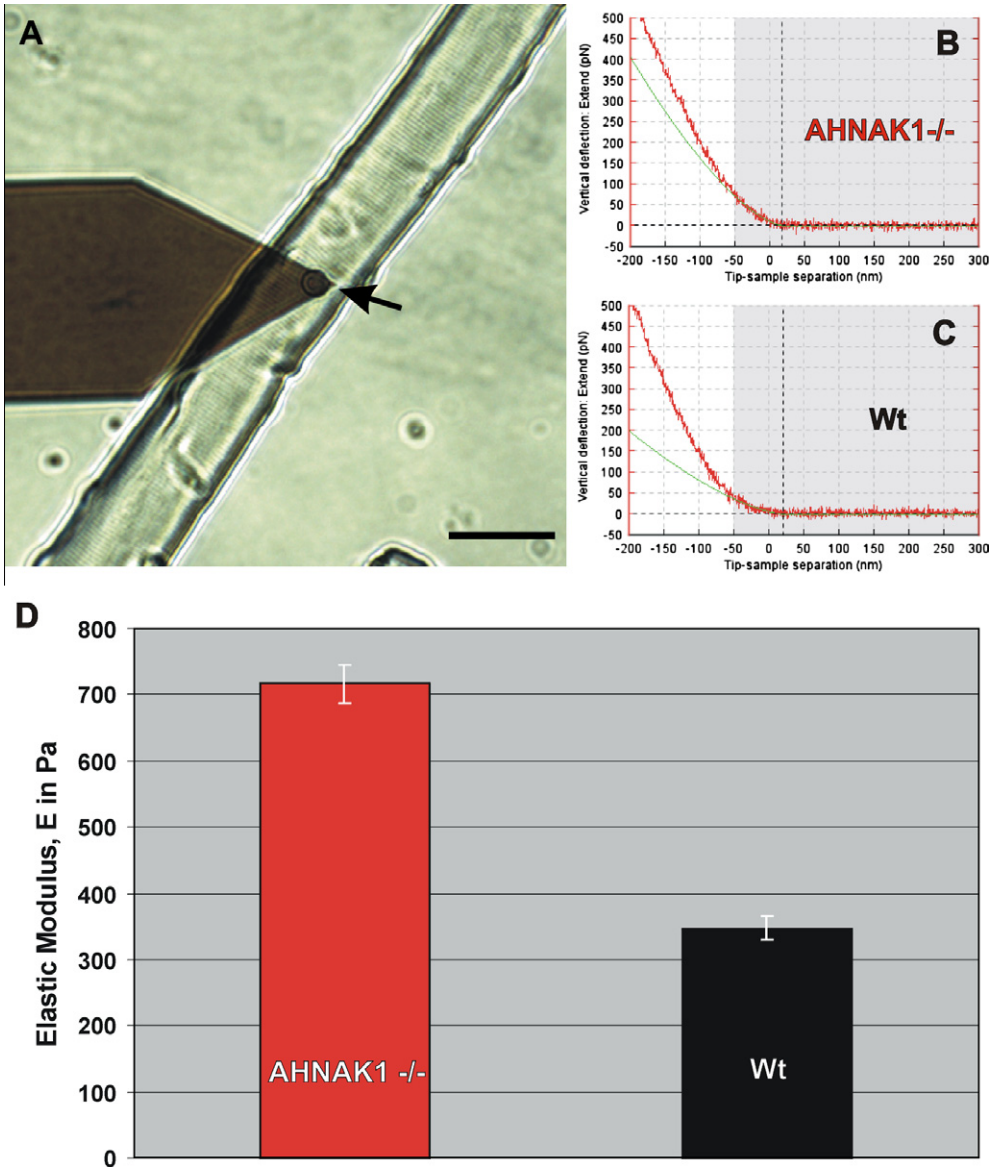

Fig. 4. AHNAK1$^{-/-}$ single fibers have a higher transverse stiffness. (A) The transverse elastic modulus of FDB muscle fibers was appointed by AFM indentation using a cantilever with an attached 11 μm-silica bead (arrow). Bar 50 μm. (B and C) Characteristic force–distance curves and corresponding Hertz fits (green lines) of an AHNAK1$^{-/-}$ fiber and a wt fiber. (D) Quantification of *E*-values. Data are means ± SEM and represent 177 measurements on 9 AHNAK1-deficient fibers and 187 measurements on 10 wt fibers. Comparison between the groups was performed using a *t* test ($P < 0.001$).

assumption. After membrane damage by laser irradiation, we analyzed FM1-43FX fluorescent dye entry into AHNAK1$^{-/-}$- and wt fibers. In the presence of Ca^{2+}, both fiber-types show only a low dye inflow (Fig. 3B and C) due to rapid membrane resealing. Membrane resealing kinetics of mouse AHNAK1$^{-/-}$ fibers were not significantly different from wt fibers (Fig. 3A). Control-experiments in the absence of Ca^{2+} clearly show an unopposed fluorescent dye entry into AHNAK1$^{-/-}$- and wt fibers as a result of an inactive membrane repair process (Fig. 3D and E). Taken together, Ca^{2+}-dependent resealing after laser induced membrane wounding clearly demonstrates an intact membrane repair process in AHNAK1$^{-/-}$ fibers and makes a functional role of AHNAK1 in membrane repair process of skeletal muscle fibers less probably.

3.4. AHNAK1$^{-/-}$ single fibers have a higher transverse stiffness

Costameres are physical links between the sarcolemma and the Z-disks. To analyze the effect of AHNAK1 on transverse fiber stiffness, we used AFM. To reduce the impact of regional fiber inhomogeneity [22], we employed an AFM-cantilever with an attached 11 μm-silica bead in force spectroscopy measurements (Fig. 4A). Standard force-distance curves were taken under identical conditions for AHNAK1$^{-/-}$- and wt fibers (Fig. 4B and C). To characterize the fiber stiffness in the region of the sarcolemma, where the AHNAK1 protein is localized, we set the fit range of the force-distance curves to 50 nm of indentation. Longer fit ranges, corresponding to the region of myofibrils, show significant higher stiffness values. In this region below the costameres we do not find differences in membrane fiber stiffness between wt- and AHNAK1$^{-/-}$ fibers.

For an indentation of 50 nm, we calculate an Elastic modulus (E) of about 700 Pa for AHNAK1-deficient fibers, which is significantly ($P < 0.001$) higher compared to the Elastic modulus of about 350 Pa for wt fibers (Fig. 4D). These data are within the range of *E*-values reported for living cells (0.1–10 kPa) [23]. Our findings demonstrate that FDB-fibers from AHNAK1$^{-/-}$ mice have a significant higher transverse stiffness than fibers from wt mice. This difference gives a first evidence for AHNAK1 function as an elastic element in the costameres. As well a role of AHNAK1 as an 'elastic bridge' between the costameres and Z-disk proteins is possible.

In summary, our results demonstrate the exclusive expression of AHNAK1 and AHNAK2 in the costameres of adult skeletal muscles. AHNAK1 is dispensable for membrane repair after laser irradiation but plays a role in transversal fiber stiffness. These findings give new indications to the functions of AHNAK in skeletal muscles. The molecular mechanisms underlying the anchoring of AHNAK in the costameres remain to be resolved.

Acknowledgments

The authors are grateful to Dr. Franz Hofmann and Dr. Peter van der Ven for providing us with antibodies. This work was supported by Deutsche Forschungsgemeinschaft Grant Clinical Research Unit 192.

Appendix A. Supplementary data

Supplementary data associated with this article can be found, in the online version, at doi:10.1016/j.bbrc.2010.09.030.

References

[1] A. Komuro, Y. Masuda, K. Kobayashi, R. Babbitt, M. Gunel, R.A. Flavell, V.T. Marchesi, The AHNAKs are a class of giant propeller-like proteins that associate with calcium channel proteins of cardiomyocytes and other cells, Proc. Natl. Acad. Sci. USA 101 (2004) 4053–4058.
[2] J. Kudoh, Y. Wang, S. Minoshima, T. Hashimoto, M. Amagai, T. Nishikawa, E. Shtivelman, J.M. Bishop, N. Shimizu, Localization of the human AHNAK/desmoyokin gene (AHNAK) to chromosome band 11q12 by somatic cell hybrid analysis and fluorescence in situ hybridization, Cytogenet. Cell Genet. 70 (1995) 218–220.
[3] E. Shtivelman, J.M. Bishop, The human gene AHNAK encodes a large phosphoprotein located primarily in the nucleus, J. Cell Biol. 120 (1993) 625–630.
[4] T. Pawson, J.D. Scott, Signaling through scaffold, anchoring, and adaptor proteins, Science 278 (1997) 2075–2080.
[5] B.J. Gentil, C. Delphin, C. Benaud, J. Baudier, Expression of the giant protein AHNAK (desmoyokin) in muscle and lining epithelial cells, J. Histochem. Cytochem. 51 (2003) 339–348.
[6] Y. Huang, S.H. Laval, A. van Remoortere, J. Baudier, C. Benaud, L.V. Anderson, V. Straub, A. Deelder, R.R. Frants, J.T. den Dunnen, K. Bushby, S.M. van der Maarel, AHNAK, a novel component of the dysferlin protein complex, redistributes to the cytoplasm with dysferlin during skeletal muscle regeneration, FASEB J. 21 (2007) 732–742.
[7] A. Hohaus, V. Person, J. Behlke, J. Schaper, I. Morano, H. Haase, The carboxyl-terminal region of ahnak provides a link between cardiac L-type Ca2+ channels and the actin-based cytoskeleton, FASEB J. 16 (2002) 1205–1216.
[8] H. Haase, J. Alvarez, D. Petzhold, A. Doller, J. Behlke, J. Erdmann, R. Hetzer, V. Regitz-Zagrosek, G. Vassort, I. Morano, Ahnak is critical for cardiac Ca(V)1.2 calcium channel function and its beta-adrenergic regulation, FASEB J. 19 (2005) 1969–1977.
[9] D. Matza, A. Badou, K.S. Kobayashi, K. Goldsmith-Pestana, Y. Masuda, A. Komuro, D. McMahon-Pratt, V.T. Marchesi, R.A. Flavell, A scaffold protein, AHNAK1, is required for calcium signaling during T cell activation, Immunity 28 (2008) 64–74.
[10] M. Kouno, G. Kondoh, K. Horie, N. Komazawa, N. Ishii, Y. Takahashi, J. Takeda, T. Hashimoto, Ahnak/desmoyokin is dispensable for proliferation, differentiation, and maintenance of integrity in mouse epidermis, J. Invest. Dermatol. 123 (2004) 700–707.
[11] H. Haase, G. Wallukat, V. Flockerzi, W. Nastainczyk, F. Hofmann, Detection of skeletal muscle calcium channel subunits in cultured neonatal rat cardiac myocytes, Recept. Channels 2 (1994) 41–52.
[12] C. Cai, H. Masumiya, N. Weisleder, N. Matsuda, M. Nishi, M. Hwang, J.K. Ko, P. Lin, A. Thornton, X. Zhao, Z. Pan, S. Komazaki, M. Brotto, H. Takeshima, J. Ma, MG53 nucleates assembly of cell membrane repair machinery, Nat. Cell Biol. 11 (2009) 56–64.
[13] J.L. Hutter, J. Bechhoefer, Calibration of atomic-force microscope tips, Rev. Sci. Intrum. 64 (1993) 1868–1873.
[14] H. Hertz, Über die Berührung fester elastischer Körper, J. für die reine und angewandte Mathematik 92 (1881) 156–171.
[15] I. Sneddon, The relation between load and penetration in the axisymmetric Boussinesq problem for a punch of arbitrary profile, Int. J. Eng. Sci. 3 (1965) 47–57.
[16] T. Masuda, N. Fujimaki, E. Ozawa, H. Ishikawa, Confocal laser microscopy of dystrophin localization in guinea pig skeletal muscle fibers, J. Cell Biol. 119 (1992) 543–548.
[17] W.M. Obermann, M. Gautel, F. Steiner, P.F. van der Ven, K. Weber, D.O. Furst, The structure of the sarcomeric M band: localization of defined domains of myomesin, M-protein, and the 250-kD carboxy-terminal region of titin by immunoelectron microscopy, J. Cell Biol. 134 (1996) 1441–1453.
[18] J.M. Ervasti, Costameres: the Achilles' heel of Herculean muscle, J. Biol. Chem. 278 (2003) 13591–13594.
[19] J.V. Pardo, J.D. Siliciano, S.W. Craig, A vinculin-containing cortical lattice in skeletal muscle: transverse lattice elements ("costameres") mark sites of attachment between myofibrils and sarcolemma, Proc. Natl. Acad. Sci. USA 80 (1983) 1008–1012.
[20] G. Ayalon, J.Q. Davis, P.B. Scotland, V. Bennett, An ankyrin-based mechanism for functional organization of dystrophin and dystroglycan, Cell 135 (2008) 1189–1200.
[21] D. Bansal, K. Miyake, S.S. Vogel, S. Groh, C.C. Chen, R. Williamson, P.L. McNeil, K.P. Campbell, Defective membrane repair in dysferlin-deficient muscular dystrophy, Nature 423 (2003) 168–172.
[22] E. Defranchi, E. Bonaccurso, M. Tedesco, M. Canato, E. Pavan, R. Raiteri, C. Reggiani, Imaging and elasticity measurements of the sarcolemma of fully differentiated skeletal muscle fibres, Microsc. Res. Tech. 67 (2005) 27–35.
[23] P.P. Girard, E.A. Cavalcanti-Adam, R. Kemkemer, J.P. Spatz, Cellular chemomechanics at interfaces: sensing, integration and response, Soft Matter 3 (2007) 307–326.